

## Evaluation and characterization of composite coating on ceramic substrate by using dip coating method

Mena F.Khdheer<sup>1, a</sup>

<sup>1, a</sup>Department of Materials Engineering / University of Technology, Bagdad, Iraq.

130014 @uotechnology.edu.iq

### Abstract

In this study, a composite coating of polyurethane resin with (CaSO<sub>4</sub>) was prepared using different proportions of ceramic powders (0, 5, 10, 15 and 20 wt.%) as a strengthening technique in the polymer matrix using adventitious coating on the ceramic substrate. Micro-hardness, porosity, FTIR, SEM, and microstructure of the composite surface were performed. Mechanical properties (hardness test) know that the highest value (88) is obtained at 15 wt % calcium carbonate. In addition, the structure testing results of both SEM and optical microscopy images of the coating revealed good cohesion and uniformity in the distribution of the ceramic powder, indicating that the composite coating structures are dense, compact, coating is around (500 nm) thick while the mean particles size distribute in to (83.01 μm) and (213.67 μm) and do not contain significant porosity value (3.2%) appear at (20 wt.% CaSO<sub>4</sub>) of carbonate compared to the uncoated sample (18%) .

**Keywords:-** CaSO<sub>4</sub>, Polyurethane, Composite material, Dip-coating, Mechanical properties

**تقييم وتوصيف الطلاء المترابك على قواعد سيراميكية باستعمال طريقة الغمس**

ميناء فيصل خضير

في هذه الدراسة تم تحضير طلاء مركب من راتنج البولي يوريثان مع (CaSO<sub>4</sub>) باستخدام نسب وزنية مختلفة من مساحيق السيراميك (0، 5، 10، 15 و 20٪ بالوزن) كتقنية طور التقوية في مصفوفة البوليمر باستخدام طلاء مغمس. على الركيزة السيراميك. تم إجراء اختبارات الصلابة الدقيقة والمسامية و FTIR و SEM والبنية المجهرية للسطح المركب. أظهرت الخواص الميكانيكية (اختبار الصلابة) أن أعلى قيمة (88) تم الحصول عليها عند 15% وزناً من كربونات الكالسيوم. بالإضافة إلى ذلك، كشفت نتائج اختبار البنية لكل من صور SEM والصور

المجهرية للطلاء عن تماسك جيد وانتظام في توزيع مسحوق السيراميك، مما يشير إلى أن هياكل الطلاء المركبة كثيفة ومضغوطة ولا تحتوي على مسامية كبيرة حيث بلغت أقل قيم للمسامية (3.2%) عند نسبة (CaSO<sub>4</sub> 20 wt%) وزناً من كربونات الكالسيوم مقارنة مع العينة بدون طلاء (18%).

## **INTRODUCTION**

Polymeric coatings are paints specially designed for the alteration and protection of substrates from corrosion due to external agents. These types of coatings can usually be applied on the substrates (surfaces) by extrusion and dispersion of the polymer [W. Harris, J (1957). Wolstenholme (1973) and J. H.Snoeijer et al.(2001)]. They may also be used to create hydrophobic surfaces and/or preventive layers against various substances or surface pollutants. Polymeric coatings are designed to have high adherence to the surfaces and a low degree of degradation and exfoliation under environmental effects such as heat, moisture, and chemical agents. The targeted alteration of the surfaces using rough-profile coatings is based on the reduction of the contact area at the surfaces (e.g. Teflon coating, PTFE, PFA, and PMMA) [J. H.Snoeijer (2001), Zhi CY et al, K. Chang et al. (2008). and J. Brown et al. (2011)]. Polymeric materials have versatile applications owing to their wide-ranging characteristics, cost-effectiveness, and ease of production and application, [M. Baglioni et al and M. Baglioni et al.(2012)]. various coating techniques, including spin and dip coatings. It is practical for thick, thin, and nanofilms to be applied on substrates at low temperatures. Dip-coating is an easy technique that can provide thick, homogeneous, crack-free coating layers that are adequate for surface protection against corrosion. Any substance that is made by shaping and then heating a nonmetallic mineral is referred to as ceramic. It is hard, brittle, heat- and corrosion-resistant. Brick, porcelain, and earthenware are typical examples. Ceramic materials' structure spans from strongly orientated to semi-crystalline, with varied crystallinity and electron density, with varying crystallinity, and electron. The majority of ceramic materials are excellent thermal and electrical insulators due to their composition in ionic and covalent bonding [T. CoanG et al.(2013)].

An effective method to enhance the qualities of polymeric coatings is to use specific filler materials with the required characteristic. The inclusion of fillers with suitable qualities are one technique to improve the properties. Through dip-coating, manufactured from composite materials of (PMMA) and hBN were created and applied to steel. Investigations were done into how the quantity of hBN in the (PMMA) coating affected corrosion resistance. For the purpose of evaluating corrosion resistance, the created coatings were immersed in NaCl and HCl solutions. The findings demonstrated that, in comparison to pure PMMA, PMMA/hBN composite coatings increased corrosion resistance. Coatings have excellent bonding with the metallic substrate and are also free of cracks, Composites made of PMMA and polysiloxane as well as their coatings were created or Methyl methacrylate (MMA) and vinyltriethoxysilane (VTEOS) were combined to form a copolymer (PMMAVTEOS), and their matching coatings were produced by an oven-curing procedure (at 75 °C). Composite coatings displayed good adhesion, high thermal

stability, and outstanding scratch resistance **C.Peng et al.(2018)**. **Shatha R. Ahmed et al (2020)**. In an effort to lessen the water absorption property and increase the hardness and compression strength of the cement mortars, has been completed to use glass powders from three different sources (window sheet glass powder, green-colored glass powder, and brown-colored glass powders). Also, the investigation and discussion of Sika floor type (161) Polyurethane Polymer's impact on the cement mortars' water absorption, hardness, and compression. The water absorption and mechanical characteristics of the mortar specimens were found to be significantly influenced by the type of glass and the weight ratio of glass to cement. The emphasis of the current studies is on the value and benefits of using ceramic particles and polyurethane polymer in the synthesis of ceramic composite application with improved properties. The effectiveness of different adhesives used to bond the reinforcing bars to the aging substrate at the rebar connections after their installation was evaluated **M. Baglioni et al (2020)** and **Al-Kaisy et al.(2020)**. According to the results, with the increase in the diameter of the rebar from (12-16) mm, the pulling load increased by (26% and 32%). The present work, it is aimed to synthesize a composite polymeric coating using polymer resin reinforced with  $\text{CaSO}_4$  (commonly known as gypsum) at different mixing ratios, their application using the dip-coating technique and investigation of their structural with mechanical properties performance.

## 1. Experimental:

Used in this work facade stone as the base material. The specimen was cut into small pieces with dimensions (20 × 20) mm, and coatings bath Polyurethane reinforced with  $\text{CaCO}_4$ , table (1) presents chemical composition of the Calcium sulfate ( $\text{CaSO}_4$ ) in different weight (0, 5, 10, 15 and 20 wt%) the ratio of additive is shown in Table (2). The specimen is dip coated with the composite mixture and left to solidify at room temperature for 72 hr. Polyurethane Sika floor (PSF) 161(1L) is reinforced with calcium sulfate (commonly known as Gypsum) particles having an average particle size of 50  $\mu\text{m}$  reinforcement of the matrix polymeric. The synthesis of the composite coating starts with the mixing of  $\text{CaSO}_4$  powder with the polyurethane resin. To maintain a uniform dispersion of the  $\text{CaSO}_4$  particles in the resin matrix, the hardening material is next added while performing continuous mixing. Ceramic substrates are then dip-coated with the composite mixture and left to solidify for (72 hr.) before characterization is performed. The weights of the samples before and after the coating process were recorded to determine the weight of the coating layers. Spectrometer for (FTIR) beams is directed toward the sample, and the amount and frequency at which the sample absorbs the light are measured. Shore-D hardness, porosity, SEM, and microstructure of the composite surface were performed.

## 2. Results and Discussion:

The FTIR spectroscope of the pure polyurethane coating in (Fig. 1a) showed that the absorption between (2992.26- 2881.05)  $\text{cm}^{-1}$  is associated with (C-H) stretching and band at (2352.93  $\text{cm}^{-1}$ ) corresponding to (NH—) stretching indicating the formation of urethane

linkages, The two resolved bands at (1696.88 and 1427.84)  $\text{cm}^{-1}$  are a result of the urethane group's carbonyl stretching, which is both hydrogen-bonded and not. While the peak at (1507.07  $\text{cm}^{-1}$ ) refers to (C=C) stretching. However, the analysis of the FTIR spectra of (PU +CaCO<sub>4</sub>) composite coating shown in (Figures 1b,c) was obtained from the composite coating /polyurethane samples. The bands at (1488, 1486, 1394.95, and 1392)  $\text{cm}^{-1}$  are indicative of various modes of (-CH<sub>2</sub>) vibrations, whereas the strong peaks at (2879  $\text{cm}^{-1}$ ). In addition, the absorption band at (1688,1722,1683 and 1724)  $\text{cm}^{-1}$  is associated with a (C=O) group in polyurethane. The bands at (1541  $\text{cm}^{-1}$ ) are used to identify the group of (NH) vibrations. The band at (1702  $\text{cm}^{-1}$ ) is attributed to hydrogen bonding between the ester or ester-oxygen groups of the soft segments of the urethane linkage and the (N-H) and (C=O) groups of the hard segment. Comparable vibrational modes with a small change were observed in the FTIR spectra of the deposited composite coatings, which are ascribed to the addition of CaCO<sub>4</sub>. Referring to the lack of any chemical interaction between the constituent parts of the composite **H. Haidar H.(2020) and H. ZA et al. (2021)**. Figure 2d shows FTIR spectra of (85%). SFS strongest spectral bands at (2991.21 and 2880.72)  $\text{cm}^{-1}$  are attributed to carbon and hydrogen bonds. The non-hydrogen-bonded carbonyl groups make up the band at (1720)  $\text{cm}^{-1}$  **Al Zuhairi et al. (2022)**. Figure (1d) shows FTIR spectra of 80%. The CH stretching is indicated by the absorption band at (2991.21  $\text{cm}^{-1}$ ).(-CH<sub>2</sub>) stretching is shown by the high peaks at (2991.21 and 2879.08)  $\text{cm}^{-1}$ . Moreover, (C=O) group in polyurethane is linked to the absorption band at (1722  $\text{cm}^{-1}$ ). The bands at (1541  $\text{cm}^{-1}$ ) serve as a marker for the NH vibrational group.

Figure (2) display scanning electron photomicrographs of the samples. The majority of the particles were flake-shaped. The coating material was successfully co-deposited on the substrate. In the composites, there was no significant agglomeration. Polyurethane CaSO<sub>4</sub> composites have a comparatively complex morphology. The polymer can form crystals, however, they do so at a somewhat sluggish rate, hence It stays primarily amorphous under typical processing settings; relatively little of it is crystallized **A. Rocha C et al.(2004)**. Along with crystalline structure, another crucial factor is the distribution of the filler in the matrix, or the potential creation of aggregates.

The coating is around (500 nm) thick and the mean particles size distribute in to (83.01  $\mu\text{m}$ ) and (213.67  $\mu\text{m}$ ) as illustrated in Figure 3, the composite coating is dense. There are no discernible borders between the interface coating and substrate coating. A good balance of dense structure, adhesion strength, and coating thickness has been demonstrated to be important for improving alloy protection. So, it can be concluded that a uniform, crack-free composite covering with a strong interface bonding might effectively lower the substrate's rate of degradation.

Figure 4 shows the relationship between the wt % of CaCO<sub>4</sub> in polymer composite coating with shore D Hardness at different percentage within Polyurethane matrix. 5% weight percentage (ceramic powders) sample, the low hardness as compared with (15% and 20%) CaCO<sub>4</sub> composite coating. The results have been shown that the hardness of the coating increase from (69) of PU pure coating to (88) of (15 % CaCO<sub>4</sub>) composite coating as shown

in Figure (4). The improvement in hardness is due to the matrix and ceramic binder's compatibility and bonding strength, which results in a more rigid surface by impeding matrix motion along the stress path. **M.**

**Mohammed et al.(2018)**. The hardness increases when the percentage of CaCO<sub>4</sub> ceramic particles increasing until 20%, this result shows the high compatibility between CaCO<sub>4</sub> and matrix binder (PL), which lead to making them harder. When it contains ceramic powder 80% in composition content will increase more than 70% of ceramic powder this effect on the strength materials. Figure (5) shows the relationship between porosity and composite coating on a ceramic substrate, Polyurethane matrix, and (ceramic binder) at room temperature. It can be noticed that the values of porosity of coating mainly depend on the % of penetration CaCO<sub>4</sub> powders in the coating layers. It of the mixture increases with an increase in CaCO<sub>4</sub> content from (5) to (20), for 20% CaCO<sub>4</sub> as is showed in figure (5). This might be attributed to the addition of the ceramic binder to polymer coating; many of the gaps and voids that existed inside the matrix would be diminished or filled by this binder, resulting in an enhancement in the prepared specimens' proportion of porosity.

**Conclusions:**

Composite coating (CaSO<sub>4</sub> with PU) was uniformly dispersed in a polymer matrix, and the addition of gypsum powder made the surface of the films rough. Improving the hardness value with an increasing weight percentage of ceramic particles or content of CaSO<sub>4</sub> particles within the polyurethane matrix. The hardness increases when the percentage of CaCO<sub>4</sub> ceramic particles increasing until 20%, this result shows the high compatibility between CaCO<sub>4</sub> and matrix binder (PU), when it contains ceramic powder 80% in composition content will increase more than 70% of ceramic powder this effect on the strength materials. This might be attributed to the addition of the ceramic binder to polymer coating; many of the gaps and voids that existed inside the matrix would be diminished or filled by this binder, resulting in an enhancement in the prepared specimens' proportion of water absorption.

**Table 1:** Chemical composition of Calcium sulfate (**M. Sudhakar et al 2009**)

Constituents	CaSO <sub>4</sub> .2H <sub>2</sub> O	SiO <sub>2</sub>	FeO <sub>3</sub> & Al <sub>2</sub> O <sub>3</sub>	Ca (OH)	MgO	pH
Mass	90	0.9	1.4	7.5	2.7	<b>9.01</b>

**Table 2:** composite coating of Polyurethane reinforced with CaCO<sub>4</sub> in different

Ratio	PU	CaCO <sub>4</sub>
Ratio 1	100 %	-
Ratio 2	95 %	5 %
Ratio 3	90%	10 %
Ratio 4	85 %	15 %
Ratio 5	80 %	20 %

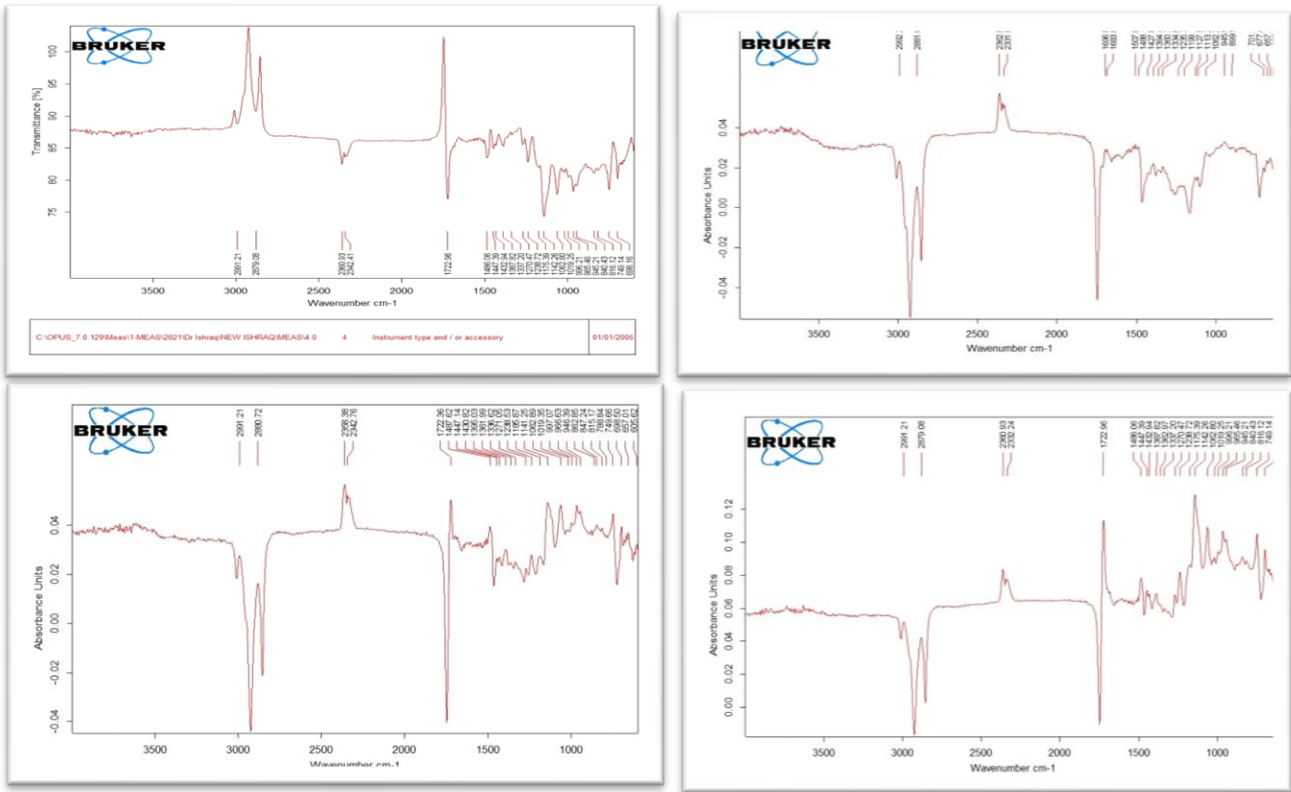


Figure (1): FTIR spectra of (a) Pure PU (b) PU + 5% CaSO<sub>4</sub> (c) PU + 10% CaSO<sub>4</sub> (d) PU + 20% CaSO<sub>4</sub>

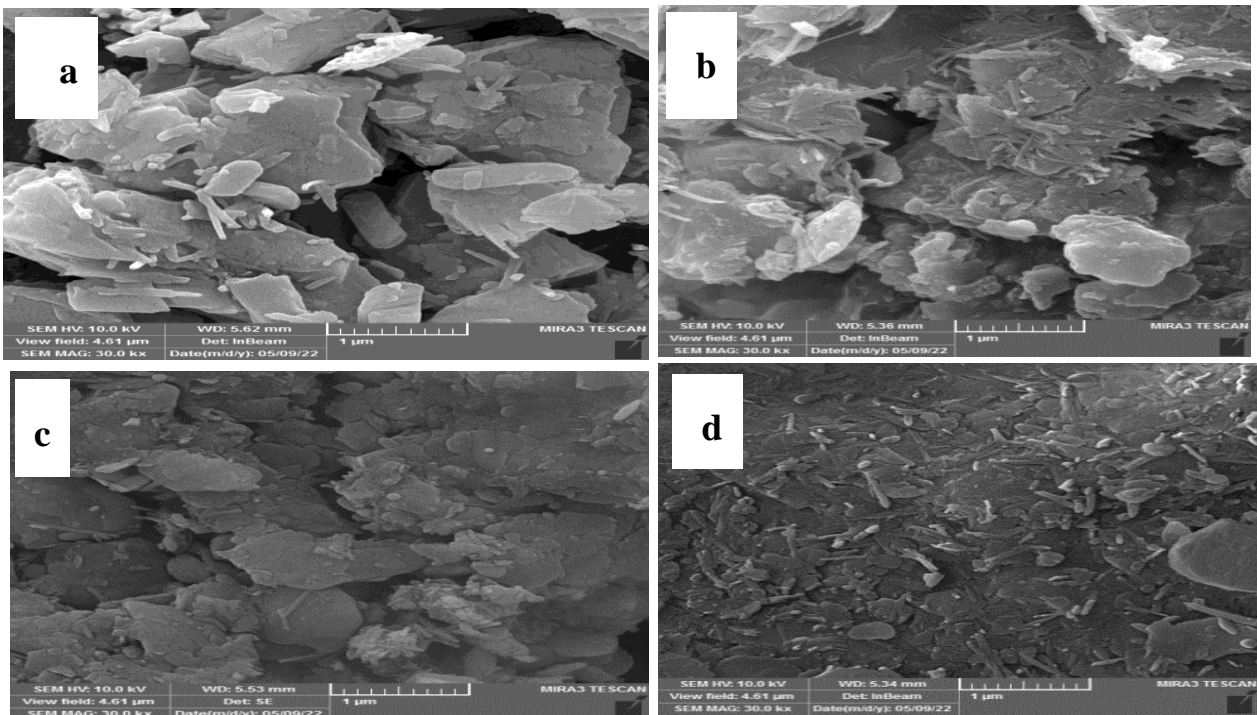


Figure (2): Typical scanning electron microscopy images of (a) Pure PU (b) PU + 5% CaSO<sub>4</sub> (c) PU + 10% CaSO<sub>4</sub> (d) PU + 20% CaSO<sub>4</sub>

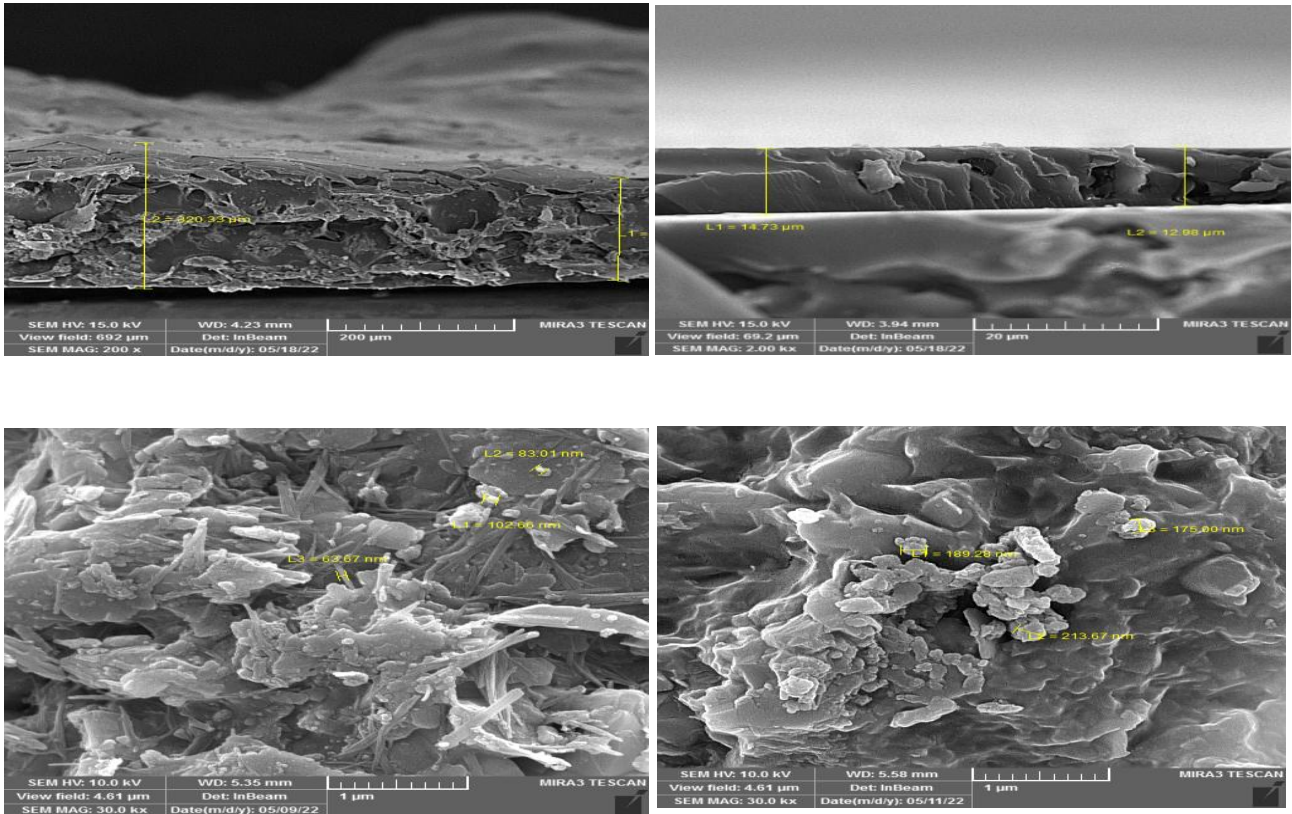


Figure (3): Cross Section and Average Diameter of composite of Coating.

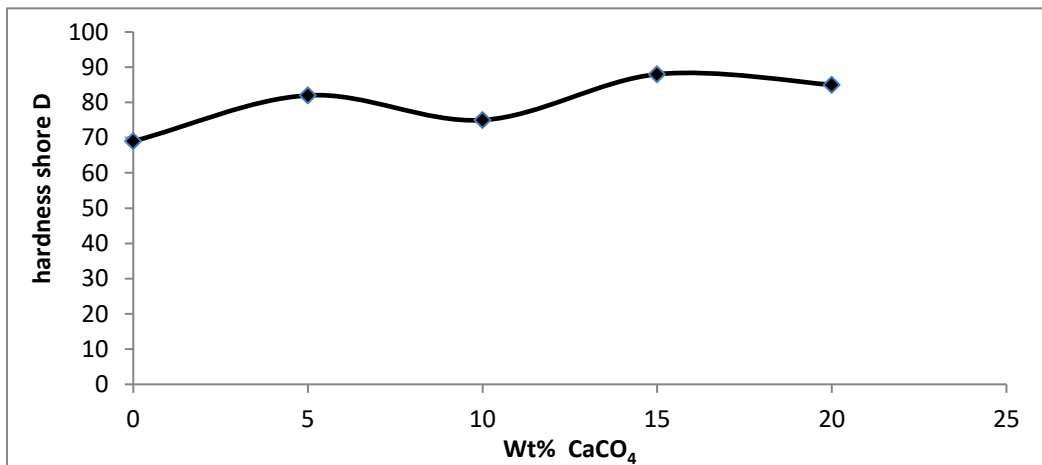


Figure (4): The microhardness of composite coating (CaCO<sub>4</sub>/ Polyurethane ) composite coating on a ceramic substrate.

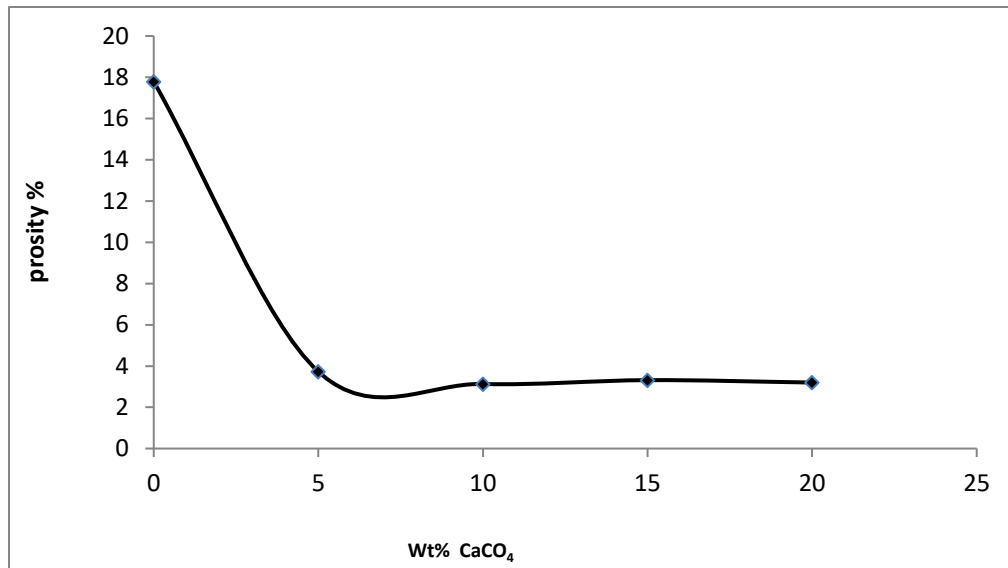


Figure (5 ): The variation of Porosity values of composite coating (CaCO<sub>4</sub>/ Polyurethane ) on ceramic substrate.

## References

W. Harris, **Corrosion, its Causes, Cost and Prevention: A Brief History of the Growth of Corrosion Study**. Anti-Corros. Methods Mater.no.4, pp.162-164, (1957).

J. Wolstenholme, , **Electrochemical methods of assessing the corrosion of painted metals-A review**. Corros. Sci.13, pp.521-530, (1973).

J. H.Snoeijs, J. Ziegler, B.Andreotti, M. Fermigier M and J. Eggers , **Thick Films of Viscous Fluid Coating a Plate Withdrawn from a Liquid Reservoir**. Physical Review Letters , no.100 (244502), pp.1-4,(2001).

Zhi CY, Bando Y, Wang WL, Tang CC, Kuwahara H and Golber D. **Mechanical and Thermal Properties of Polymethyl Methacrylate-BN Nanotube Composites**. Journal of Nanomaterials, vo.18, pp. 1-5,(2008).

J. Brown, R. **Evaluation of Protective Coatings for Ship Bottoms**. Corrosion ,vo.15, pp.49-54, (2009).

M. Kiran, K. Raidongia, U.Ramamurty and C.Rao ,**Improved mechanical properties of polymer nanocomposites incorporating graphene-like BN: Dependence on the number of BN layers**. Scripta Materialia ,vo.64, pp.592-595, (2011).

M. Baglioni, D. Berti, J. Teixeira, R. Giorgi, and P. Baglioni, **Nanostructured surfactant-based systems for the removal of polymers from wall paintings: a small-angle neutron scattering study**. Langmuir 28, pp. 15193-15202, (2012).

M. Baglioni, J. Benavides, Y., D.Drapela, A., and R. Giorgi, **Amphiphile-based nanofluids for the removal of styrene/acrylate coatings: cleaning of stucco decoration in the Uaxactun archeological site (Guatemala)**. J. Cult. Herit. 16, pp. 862-868, (2012b).

Yeh J, Liou S, Lai M, Chang Y, Huang C, Chen C et al. **Comparative studies of the properties of poly(methyl methacrylate) - clay nanocomposite materials prepared by in situ emulsion polymerization and solution dispersion**. Journal of Applied Polymer Science ,vo.94, pp.1936-1946, (2004).

K. Chang, S.Chen, H. Lin, C.Lin, H. Huang, J.Yeh, **Effect of clay on the corrosion protection efficiency of PMMA/Na<sup>+</sup>-MMT clay nanocomposite coatings evaluated by electrochemical measurements**. European Polymer Journal ,vo.44, pp.13-23, (2008).

M. Sudhakar Rao<sup>1</sup>, G. C. Raju and B. V. Venkatrama Reddy, **Compressive strength behavior of calcined gypsum sludge-sand specimens**, International Journal of Geotechnical Engineering vo.3: pp. 65-73, (2009), DOI 10.3328/IJGE.2009.03.01.pp.65-73

T. Coan G. S. Barroso G. Motz A. Bolzán R. A. F. Machado **Preparation of PMMA/hBN Composite Coatings for Metal Surface Protection**, Regular Articles ,Mat. Res.vo. 16 no.6 , Dec ( 2013).

[C.Peng X.](#), [H.Ting](#) , [J.Yin P.](#), **Synthesis and characterization of poly(methyl methacrylate)/polysiloxane composites and their coating properties**, Wiley Periodicals, Inc. J. Appl. Polym. Sci.vo.135, pp. 46358, (2018).

A.Al-Kaisy Hanaa, M. Salih Shaymaa, Al-Gebory Layth, **Preparation And characterization of TiO<sub>2</sub>-ZrO<sub>2</sub> coating Prepared by Sol-Gel Spin Method**, The Iraqi Journal For Mechanical And Material Engineering,vo.20, no3,Sept.(2020).

R.A.Shatha, F.K.Mena. , B. Al-Zubaidi Aseel, **The Mechanical Properties of Green Cement Mortar Dip-Coated with Polyurethane Polymer**, Journal of Mechanical Engineering Research and Developments ISSN: 1024-1752, vo. 43, no. 2, pp. 239-246, ( 2020).

H. [Haidar H.](#),[I.Faten](#) , [A. Mussa](#),[O. Dawood](#), [A. Ahmed A.](#) and [A. Rassel G.](#),  
**Experimental Study of Post Installed Rebar Anchor Systems for Concrete Structure**,  
[Civil and Environmental Engineering](#), vo. 16 - Issue 2 mpp. 308 – 319, December (2020).

H. ZA, Shakor ZM, Alzuhairi M, Al-Sheikh F. **Thermal and catalytic cracking of plastic waste: a review**. International Journal of Environmental Analytical Chemistry. vo.1,pp.11-8, (2021).

Al Zuhairi, M. ,Al-Kaisy H. , Khdheer, M. **Depolymerization of wast plastic using Bubble column for Nano Alumina Blended coating** , Fluids ,no.7,pp. 127, (2022).

A. Rocha C, F.Rizzo, C.Zeng and M.Paes. **Duplex Al-based thermal spray coatings for corrosion protection in high temperature refinery applications**. Materials Research 7, pp.189-194, (2004).

M.Mohammed., SH.Zaidan and A. Al-kasiy H.,**Investigation of Ceramic Coatingby Thermal Spray with Diffusion of Copper**”,ACTA PHYSICA POLONICA A, vo. 134,no.1 ,(2018).